Conformational Analysis by UV Spectroscopy: the Decisive Contribution of Environment-Induced Electronic Stark Effects

Jeremy Donon, Sana Habka, Michel Mons, Valérie Brenner, Eric Gloaguen

LIDYL, CEA, CNRS, Université Paris Saclay; CEA Saclay, Bât 522, 91191 Gif-sur-Yvette, France

Turbomole options

The following non-default (program define) TURBOMOLE 7.0 options were used for geometry optimization and frequency calculations at the RI-B97-D3/dhf-TZVPP level:

```
$scfconv   8
$dft
   gridsize   m4
   weight derivatives
$disp3
```

For electric field calculations at the RI-B97-D3(BJ)/def2-QZVPP//RI-B97-D3(BJ)-abc/dhf-TZVPP level, the following non-default options of TURBOMOLE 7.2 were used:

```
$scfconv   8
$dft
   gridsize   m5
   weight derivatives
$disp3 bj abc #abc when applicable
```

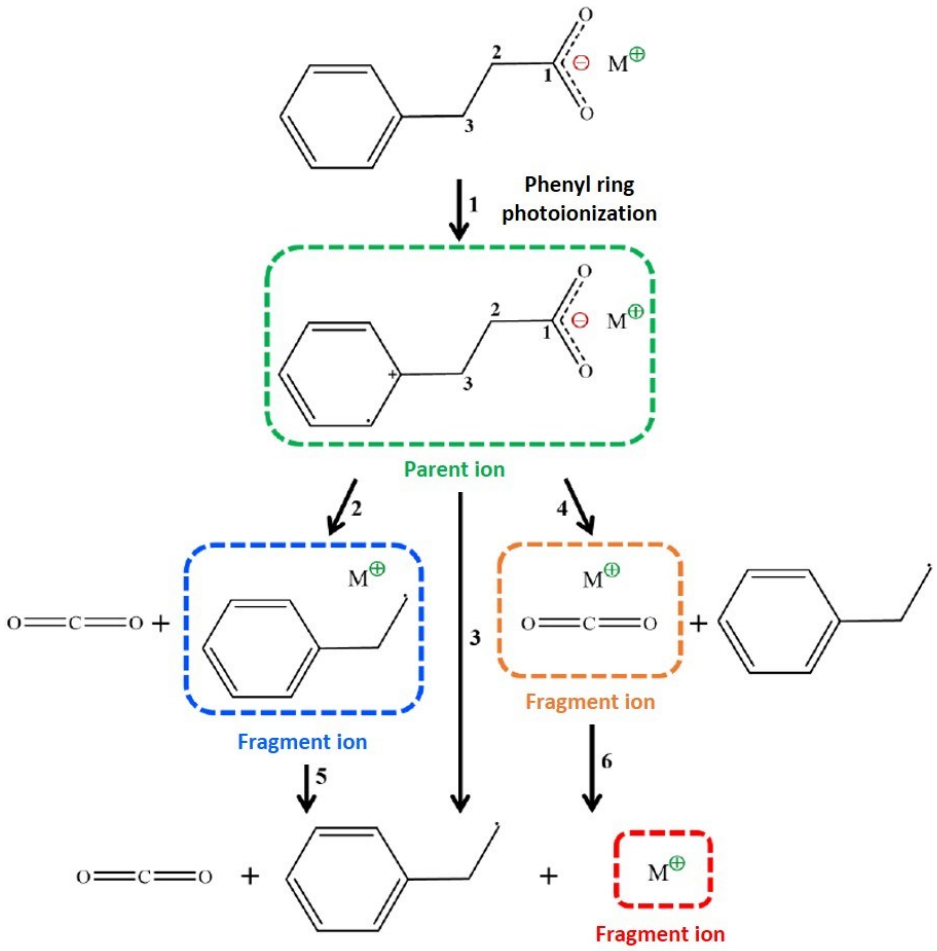

Figure S0. Reaction scheme featuring a photoinduced decarboxylation of the (M^+, BA^-) systems, consistent with the *m/z* of ions measured by mass spectrometry, *i.e.* the parent ion (green), the (parent-CO_2)$^+$ (blue), the $CO_2 \cdot M^+$ complex ion (orange), and the alkali cation M^+ (red).

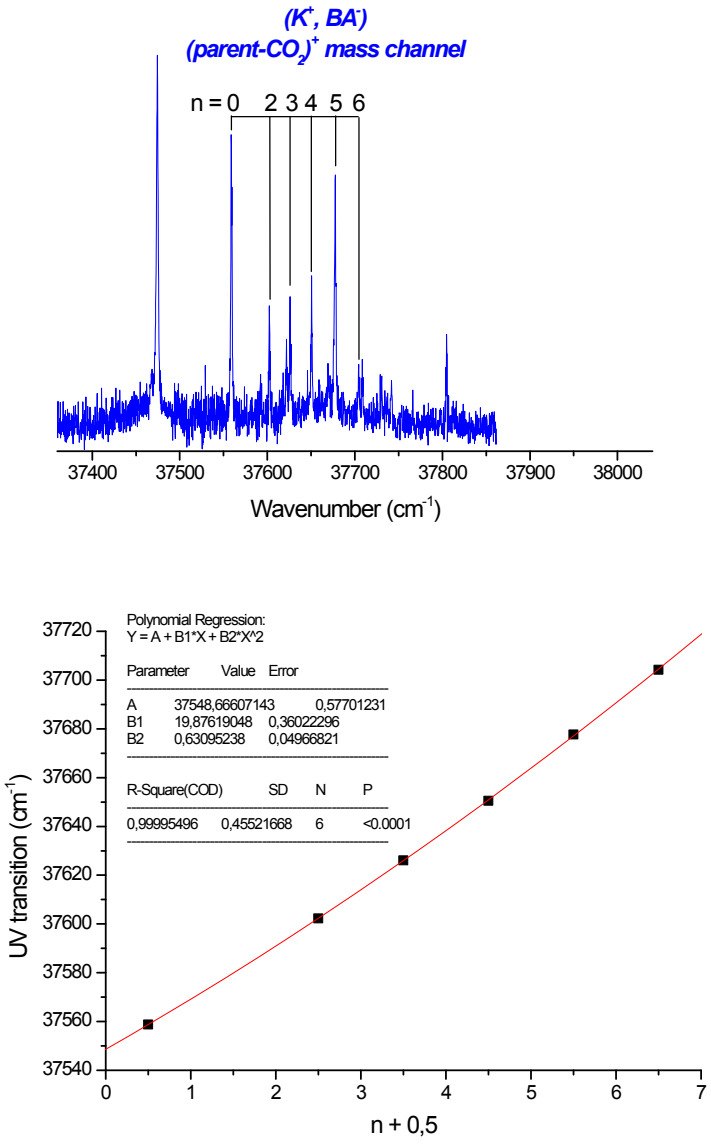

Figure S1. Top: Vibrational progression observed on the (parent-CO_2)$^+$ mass channel of the (K^+, BA^-) ion pair, for which the vibrational quantum number *n* is assigned. Bottom: Second order polynomial regression.

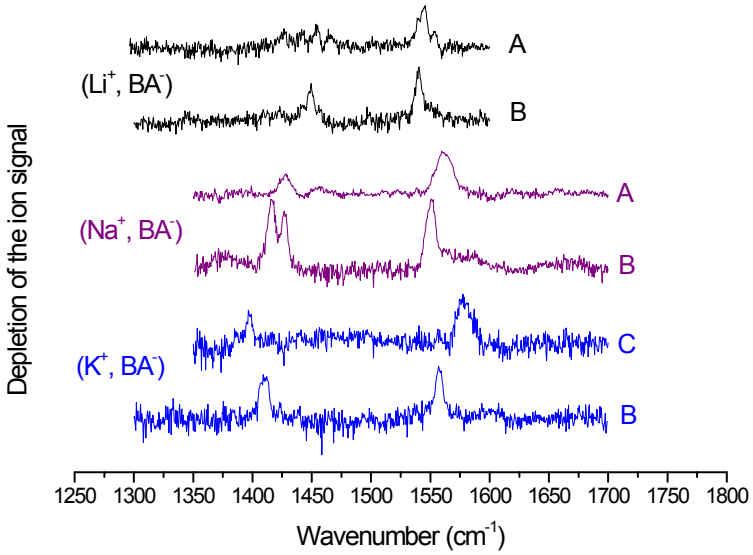

Figure S2. IR spectra recorded by the IR/UV technique at a UV wavelength corresponding to the most intense transition of the most intense mass channel (see Fig. 2) for every conformer considered along the (M^+, BA^-) series. While experimental frequencies of the CO_2^- stretch modes of both conformers **A** and **B** are very similar in (Li^+, BA^-) and (Na^+, BA^-), that of **C** are quite different from **B** in (K^+, BA^-), with a clear increase of the CO_2^- stretch modes splitting in the former.

Table S1. Comparison between theoretical mode-dependent scaled frequencies at the RI-B97-D3/dhf-TZVPP level and experimental frequencies of the CO_2^- stretch modes, $\nu(CO_2^-)^{sym/anti}$, and their difference, $\Delta\nu(CO_2^-)$ (in cm^{-1}). In case of multiplets (d for doublets, or q for quadruplets), the spectral range is given. O-O-π conformers are characterized by blue shifted $\nu(CO_2^-)^{anti}$ and a larger $\Delta\nu(CO_2^-)$ than O-O within the same system. This behavior is also observed for conformer **C** relatively to **B** for (K^+, BA^-), supporting the assignment of **C** to the **gc (O-O-π)** conformer. The evolution of $\nu(CO_2^-)^{sym}$ is considered less reliable due to the presence of couplings blurring the comparison between harmonic calculations and experiments.

	Theory					Experiment			
	Label	**Type**	**$\nu(CO_2^-)^{sym}$**	**$\nu(CO_2^-)^{anti}$**	**$\Delta\nu(CO_2^-)$**	**Conf.**	**$\nu(CO_2^-)^{sym}$**	**$\nu(CO_2^-)^{anti}$**	**$\Delta\nu(CO_2^-)$**
(Li^+, BA^-)	ap	O-O	1424	1537	113	B	1449.0	1540.5	91.5
	ac	O-O	1421	1540	119				
	gc	O-O	1433	1542	109	A	q(1426-1465)	1544.5	99[a]
	pl-ap	O-O	1425	1540	115				
(Na^+, BA^-)	ap	O-O	1392	1554	162	B	d(1416-1427)	1551	129.5[a]
	ac	O-O	1391	1553	162				
	gc[b]	O-O	1403	1556	153	A	1428.5	1561	132.5
	gc	O-O-π	1398	1569	171				
	pl-ap	O-O	1396	1554	158				
(K^+, BA^-)	ap	O-O	1382	1562	180	B	1410	1557	147
	ac	O-O	1381	1562	181				
	gc	O-O-π	1390	1579	189	C	1397	1578	181
	pl-ap	O-O	1380	1563	183				
(Rb^+, BA^-)	ap	O-O	1382	1558	176				
	ac	O-O	1381	1559	178				
	gc	O-O-π	1391	1575	184				
	pl-ap	O-O	1380	1560	180				

a. The center of the multiplet is used to calculate the difference

b. Partial optimization with a fixed $C^{ipso}C^aC^bC^c$ angle (Table 1)

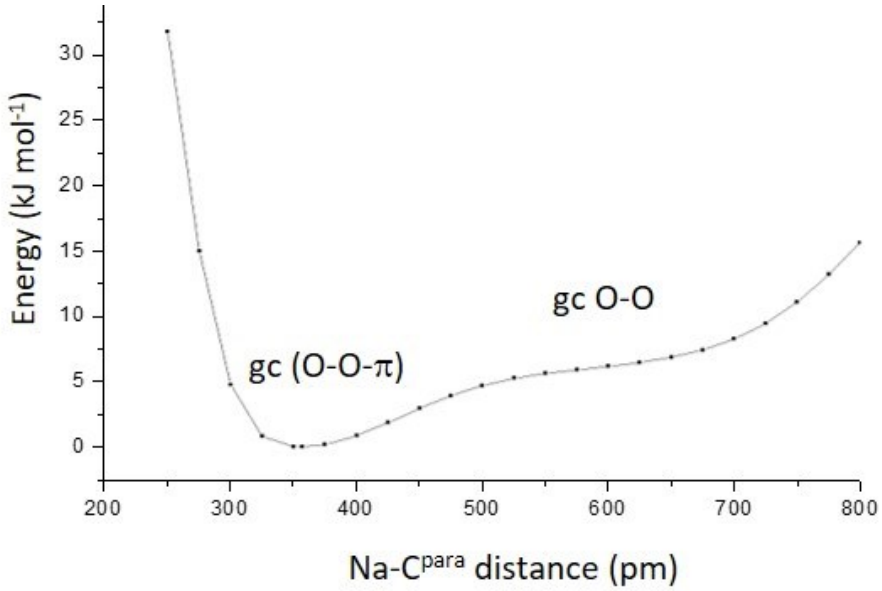

Figure S3. Energy profile of the (Na^+, BA^-) **gc** conformers along the Na-C^{para} coordinate obtained after partial optimizations at the RI-B97-D3(BJ)-abc/dhf-TZVPP. This profile shows a quite large basin, where the minimum of the potential energy surface is of O-O-π type, whereas an inflexion is seen in the region typical of O-O conformers (~600 pm). Similar results were obtained for (Li^+, BA^-) and (K^+, BA^-). The experimental observation of O-O conformers for (Li^+, BA^-) and (Na^+, BA^-) suggest that the stabilization of O-O-π conformers is overestimated by at least ~5 kJ mol^{-1} relatively to O-O conformers. This profile obtained at a rather advanced level of calculation illustrates how challenging the theoretical structural description of these systems is.

Table S2. The electric field ***E*** (in GV m^{-1}) produced by the (M^+, $^\bullet CH_2$-CH_2-CO_2^-) system, calculated at the center of the phenyl ring at the RI-B97-D3(BJ)/def2-QZVPP//RI-B97-D3(BJ)-abc/dhf-TZVPP level is presented for the (M^+, BA^-) series. The electric fields produced by the $^\bullet CH_2$-CH_2-CH_3 (resp. $^\bullet CH_2$-CH_2-COOH) system in both conformers of *n*-propylbenzene (resp. benzylacetic acid) are also shown.

		$\|\|E\|\|$	E_x	E_y	E_z
(Li^+, BA^-)	ap (O-O)	2.65	-2.64	0.00	-0.27
	ac (O-O)	2.35	-2.34	0.00	-0.14
	gc (O-O)	2.70	-2.66	0.36	-0.27
(Na^+, BA^-)	ap (O-O)	3.29	-3.29	0.00	-0.15
	ac (O-O)	3.01	-3.01	0.00	-0.02
	gc (O-O)[a]	3.40	-3.39	-0.12	-0.18
(K^+, BA^-)	ap (O-O)	3.73	-3.73	0.00	-0.06
	ac (O-O)	3.49	-3.49	0.00	0.07
(Rb^+, BA^-)	ap (O-O)	3.82	-3.82	0.00	-0.04
	ac (O-O)	3.58	-3.58	0.00	0.08
***n*-propylbenzene**	a	2.14	-2.13	0.00	-0.23
	g	2.12	-2.09	0.06	-0.39
Benzylacetic acid	ap	1.45	-1.32	0.00	0.60
	gc	1.53	-1.33	-0.60	-0.45

a. Conformer resulting from a partial optimization at the RI-B97-D3/dhf-TZVPP level (Table 1 and S1).

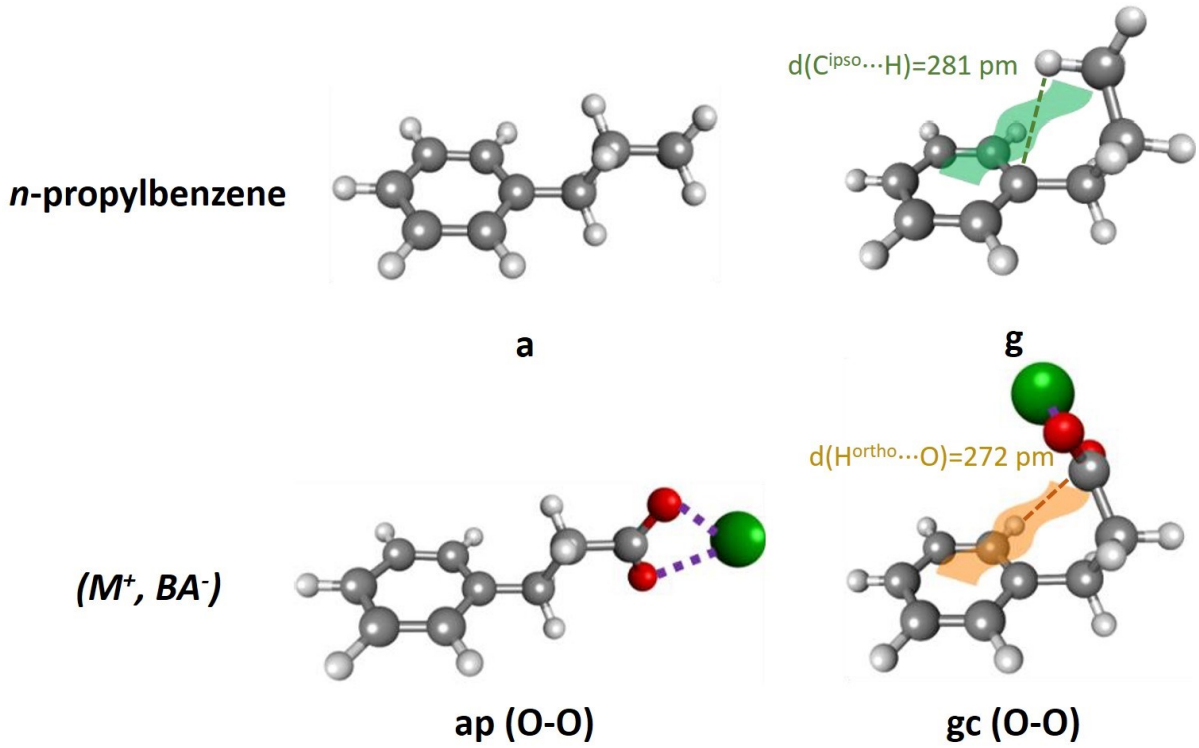

Figure S4. Interactions between the phenyl ring and the methyl (green) or the $-CO_2^-M^+$ (orange) group in *n*-propylbenzene and (M^+, BA^-) ion pairs respectively. These interactions mainly occur in conformers where the $C^{ipso}C^aC^bC^c$ angle is **g**, but not when it is **a**.

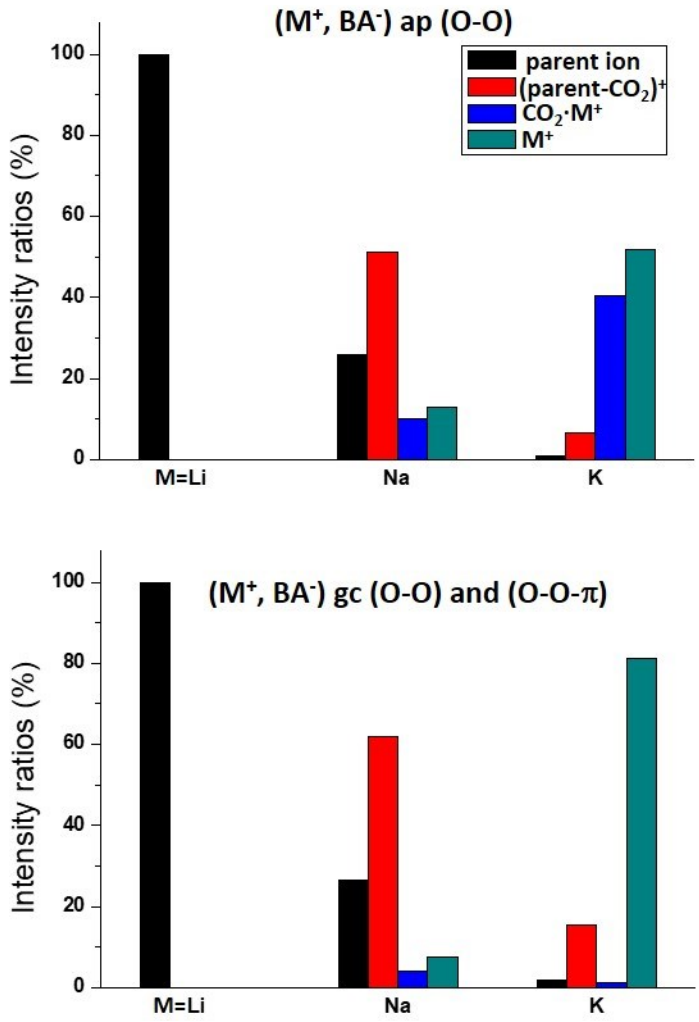

Figure S5. Ion signal intensity ratios between the different mass channels taken at the origin transitions of (M^+, BA^-) conformers **B** assigned to **ap (O-O)** (top) and **A** or **C** assigned to **gc (O-O)** or **(O-O-π)** (bottom) for M= Li, Na and K.

Table S3. Ionic bond energy of the (M^+, AcO^-) bidentate ion pairs calculated at the BSSE-corrected-Full-CCSD(T)/dhf-TZVPP//RI-B97-D3/dhf-TZVPP level[1-2] for M = Li, Na, K, Rb, Cs.[3]

System	Binding energy (kJ mol^{-1})
(Li^+, AcO^-)	708
(Na^+, AcO^-)	605
(K^+, AcO^-)	525
(Rb^+, AcO^-)	498
(Cs^+, AcO^-)	495

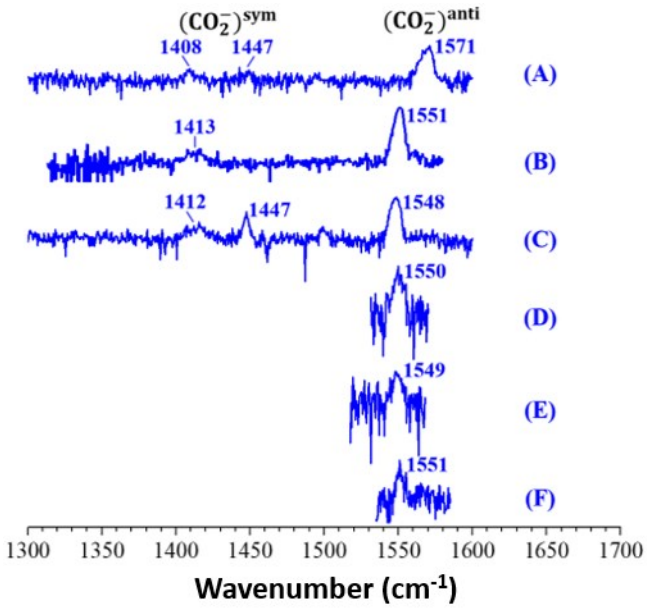

Figure S6. IR spectra recorded by the IR/UV technique at a UV wavelength corresponding to the most intense transition of the most intense mass channel (see Fig. 5) for every conformer of the (Na^+, PB^-) system. The antisymmetric transition of **A** is clearly blue-shifted by 20-23 cm^{-1} relatively to all the other conformers.

Table S4. Comparison between theoretical mode-dependent scaled frequencies at the RI-B97-D3/dhf-TZVPP level and experimental frequencies of the CO_2^- stretch modes, $\nu(CO_2^-)^{sym/anti}$ (in cm^{-1}). In case of multiplets (d for doublets, or t for triplets), the spectral range is given. O-O-π conformers are characterized by blue shifted $\nu(CO_2^-)^{anti}$ by at least 10 cm^{-1}. A ~20 cm^{-1} blueshift is also observed for conformer **A** relatively to the others, supporting the assignment of **A** to the **gg$^-$c (O-O-π)** conformer.

	Theory				Experiment		
	Label	**Type**	**$\nu(CO_2^-)^{sym}$**	**$\nu(CO_2^-)^{anti}$**	**Conf.**	**$\nu(CO_2^-)^{sym}$**	**$\nu(CO_2^-)^{anti}$**
(Li^+, PB^-)	aap	O-O	1425	1537	D	t(1417-1462)	1538
	aac	O-O	1424	1540	F		
	agp	O-O	1428	1538	C	1452	1537
	gap	O-O	1427	1535			
	gac[a]	O-O			E		1537
	ggc	O-O	1432	1535			
	gg$^-$c	O-O-π	1433	1555	A	1453	1557
	pl-aap	O-O	1426	1537	B	1447	1537
(Na^+, PB^-)	aap	O-O	1394	1555	D		1550
	aac	O-O	1395	1552	F		1551
	agp	O-O	1399	1555	C	d(1412-1447)	1548
	gap	O-O	1394	1552			
	gac[a]	O-O			E		1549
	ggc	O-O	1407	1552			
	gg$^-$c	O-O-π	1409	1568	A	d(1408-1447)	1571
	pl-aap	O-O	1395	1551	B	1413	1551

a. Partial optimization with a fixed dihedral angle around the C^cC^d bond (see Table 2)

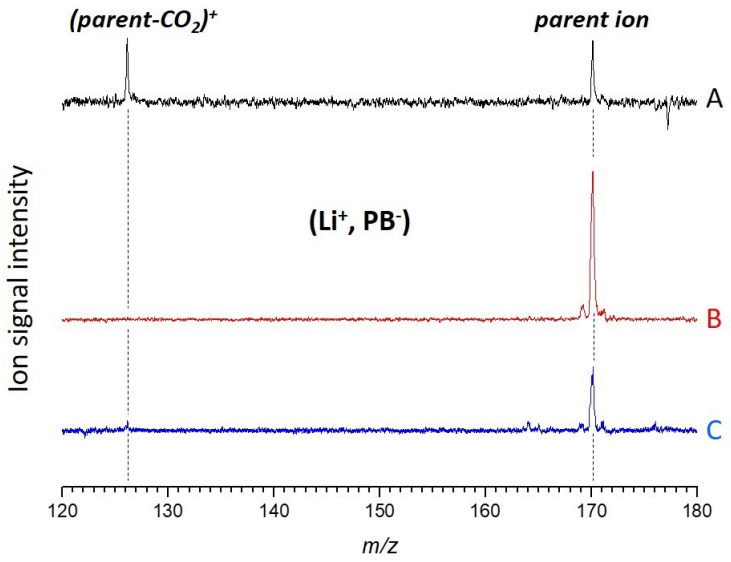

Figure S7. Mass spectra of (Li^+, PB^-) resulting from the difference between spectra taken in resonance with transitions **A B** and **C**, and off resonance. Despite the mass spectrum of conformer **B** has the highest signal-to-noise parent ion intensity, it does not show any (parent-CO_2)$^+$ signal, while this fragmentation channel is clearly detected on **A** or **C**.

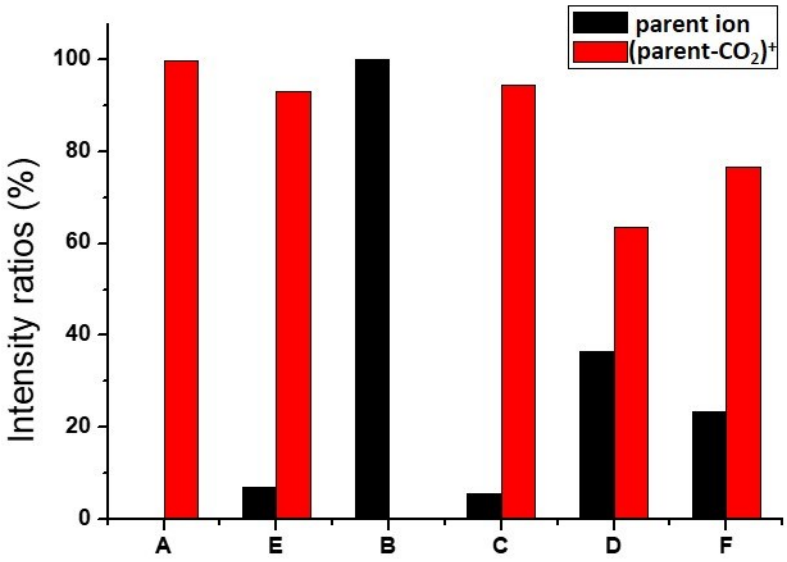

Figure S8. Ion signal intensity ratios between the parent ion and $(parent\text{-}CO_2)^+$ mass channels taken at the origin transitions of (Na^+, PB^-) conformers. Please note that the $CO_2{\cdot}Na^+$ and Na^+ channels are not taken into account.

Table S5. The electric field ***E*** (in GV m^{-1}) produced by the (M^+, $^\bullet CH_2$-CH_2-CH_2-CO_2^-) system, calculated at the center of the phenyl ring at the RI-B97-D3(BJ)/def2-QZVPP//RI-B97-D3(BJ)-abc/dhf-TZVPP level is presented for the (M^+, PB^-) series. The electric field produced by the $^\bullet CH_2$-CH_2-CH_2-CH_3 system in both conformers of *n*-butylbenzene is also shown.

		$\|\|E\|\|$	E_x	E_y	E_z
(Li^+, PB^-)	aap (O-O)	2.54	-2.54	0.00	-0.02
	aac (O-O)	2.39	-2.38	0.00	-0.18
	agp (O-O)	2.60	-2.60	0.15	-0.10
	gap (O-O)	2.35	-2.32	0.01	-0.34
	ggc (O-O)	2.40	-2.34	0.51	-0.16
	pl-aap (O-O)	2.55	-2.55	-0.02	-0.01
(Na^+, PB^-)	aap (O-O)	2.99	-2.99	0.01	0.05
	aac (O-O)	2.85	-2.84	0.01	-0.13
	agp (O-O)	3.03	-3.03	0.13	0.01
	gap (O-O)	2.72	-2.72	0.07	-0.14
	ggc (O-O)	2.84	-2.77	0.62	0.04
	pl-aap (O-O)	3.00	-3.00	0.02	0.01
***n*-butylbenzene**	aa	2.21	-2.20	0.00	-0.22
	ag	2.17	-2.16	0.01	-0.22
	ga	2.15	-2.11	0.08	-0.38
	gg	2.14	-2.10	0.02	-0.39

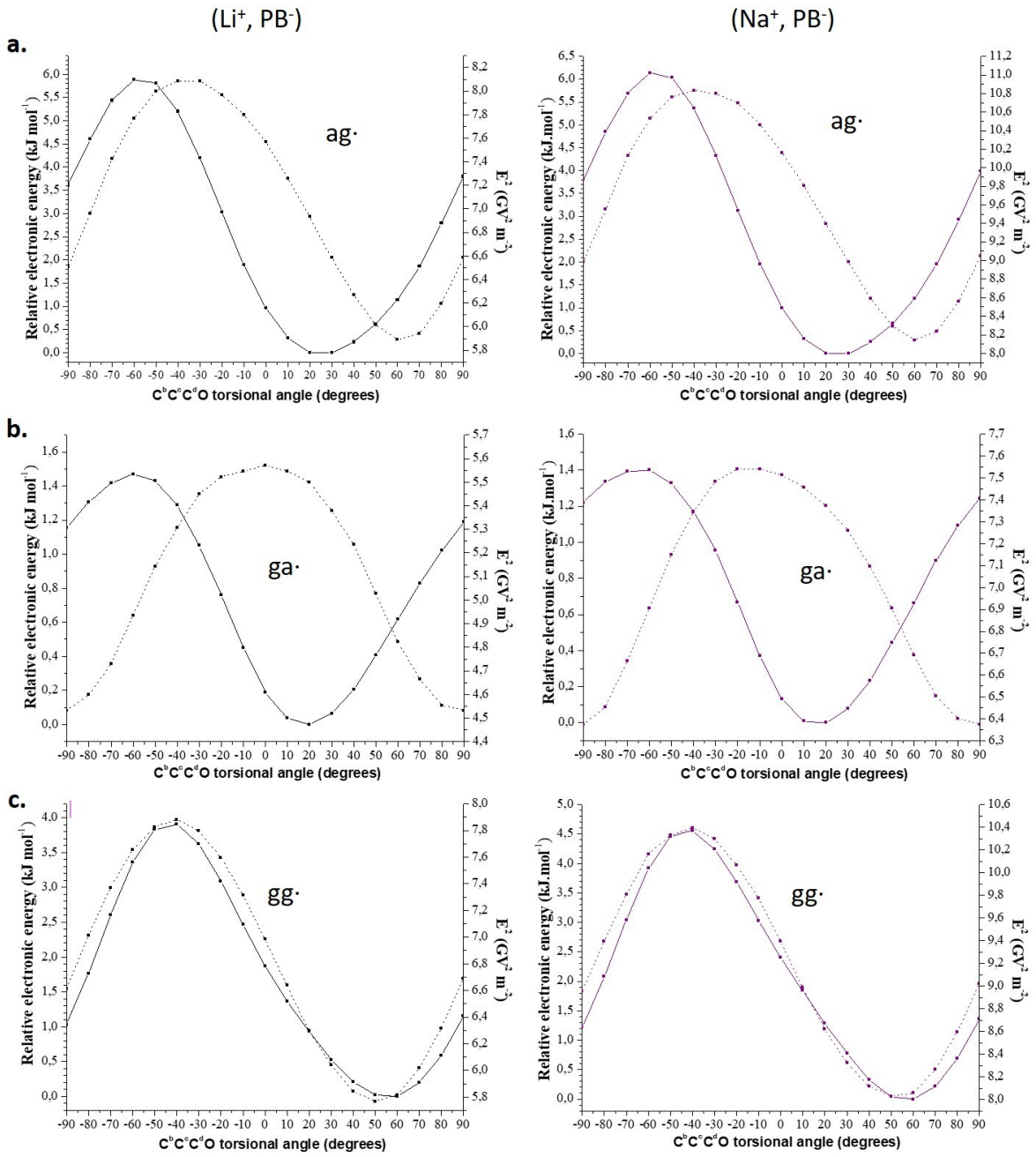

Figure S9. Energy profiles (solid lines) and electric field profiles (dotted lines) along the $C^bC^cC^dO$ dihedral angle for the ag· (a), ga· (b) and gg· (c) conformers of (Li^+, PB^-) (left) and (Na^+, PB^-) (right).

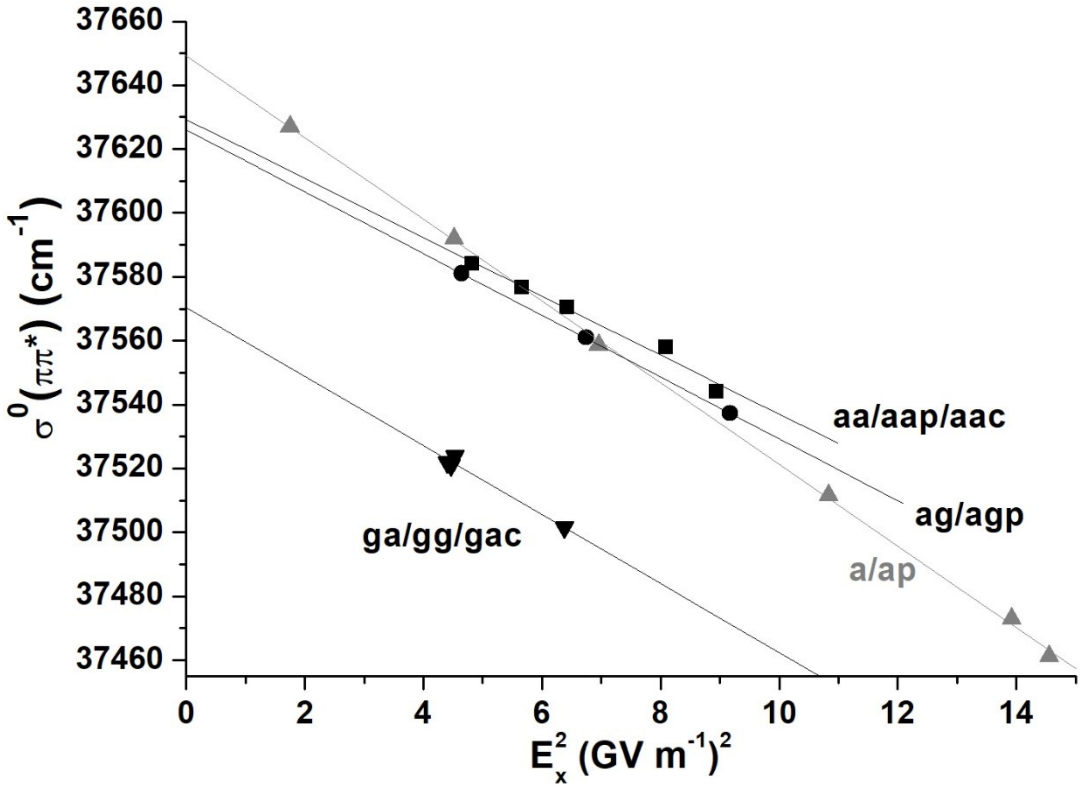

Figure S10. Experimental origin electronic transitions reported as a function of the square of the calculated electric field component E_x generated by the chain ($^{\bullet}CH_2$-R, R depending on the system) at the center of the phenyl ring for all conformers involved in a quadratic Stark effect for *n*-propylbenzene, *n*-butylbenzene, benzylacetic acid, (M^+, BA^-) for M = Li, Na, K and Rb, (Li^+, PB^-) and (Na^+, PB^-). The four sets of conformers are distinguished by their symbols and linearly fitted.

References

1. Boys, S. F.; Bernardi, F., Calculation of small molecular interactions by differences of separate total energies. Some procedures with reduced errors. *Mol. Phys.* **1970,** *19* (4), 553-566.
2. Raghavachari, K.; Trucks, G. W.; Pople, J. A.; Headgordon, M., A fifth-order perturbation comparison of electron correlation theories. *Chem. Phys. Lett.* **1989,** *157* (6), 479-483.
3. Habka, S. Spectroscopie optique de paires d'ions: De la caractérisation des modèles en phase gazeuse à l'identification des paires d'ions en solution. Université Paris-Saclay, 2017.